Photoassisted Deposition of Chalcogenide Semiconductors on the Titanium Dioxide Surface: Mechanistic and Other Aspects

Sashikala Somasundaram, C. R. Chenthamarakshan, Norma R. de Tacconi, Yong Ming, and Krishnan Rajeshwar*

Department of Chemistry and Biochemistry, The University of Texas at Arlington, Arlington, Texas 76019-0065

Received May 4, 2004. Revised Manuscript Received July 15, 2004

Heterogeneous photocatalysis using photoexcited TiO_2 substrates (either in dispersed suspensions or in thin film form) is shown to be a versatile method for preparing Se- or metal selenide (MSe)-modified TiO_2 surfaces. The mechanistic aspects underlying this novel preparative route are addressed using chronopotentiometry and linear sweep photovoltammetry. The photovoltammograms of Se/TiO_2 composite electrodes exhibit unusual "bipolar" behavior, i.e., both photocathodic and photoanodic enhancement of current flow on the same trace, depending on the imposed potential bias. This interesting photoelectrochemical behavior is rationalized on the basis of the electronic properties of the Se/TiO_2 junction. Ex situ characterization of the composite semiconductor samples was also carried out. Finally, an application of $CdSe/TiO_2$ samples for environmental remediation of Cr^{VI} is demonstrated.

Introduction

Photocatalytic processes on the titanium dioxide (TiO_2) surface have been widely deployed for the mineralization of organic pollutants[1−3] and the immobilization of toxic metal ions[1,4] in water. It occurred to us that such processes could also be exploited for the photoassisted deposition of targeted chalcogenide semiconductors on the oxide surface. Indeed, there is precedence for the photocatalytic deposition of metals and polymers on oxide semiconductor surfaces. Thus, optical excitation of aqueous TiO_2 slurries was used to modify the oxide surface with noble metal (e.g., Pt) catalyst islands.[5] Photopolymerization of both styrene and methyl methacrylate monomer was noted on TiO_2 when light was focused on the oxide semiconductor.[6] Polypyrrole was photodeposited on ZnO[7] and on aqueous dispersions of TiO_2 powder.[8,9] In most of these cases, a reducing agent (e.g., acetate) was used in the aqueous medium (contacting the oxide surface) to scavenge the photogenerated holes.

In an earlier communicaton,[10] we showed that a TiO_2 surface previously modified with selenium could be used to subsequently prepare MSe/TiO_2 (M = Cd, Pb) composite semiconductors. In this paper, we describe the mechanistic aspects of this MSe deposition process using both in situ (photovoltammetry, chronopotentiometry) and ex situ (electron probe microanalysis, X-ray photoelectron spectroscopy) measurement probes. Photoassisted deposition of Se or MSe was carried out both in aqueous dispersions of TiO_2 and on TiO_2 film substrates. Interesting "bipolar" photoelectrochemical behavior[11] was exhibited by the resultant composite semiconductor electrode structures.

Experimental Section

Chemicals and Materials. The TiO_2 (Degussa P-25) used was predominantly anatase and had a specific surface area of ~60 m^2/g. Selenium(IV) oxide (Johnson Mathey, 99.9%), cadmium sulfate (Aldrich, 99.8%), and lead chloride (Aldrich, 99.8%) were used without further purification. [**CAUTION**: Selenium, cadmium, and lead solutions are toxic; their handling and disposal must be done with extreme care]. All other chemicals were at least reagent grade and were used without further purification. Deionized (18 MΩ) water was used in all the cases for making solutions.

The TiO_2 films were made by dip-coating gold foils (~100 mm^2 area and 0.25 mm thickness, Alfa Aesar) in the Degussa P-25 TiO_2 suspensions (2-propanol containing 10 g/L oxide dose) after carefully masking one side with cellophane tape. After the dip, the foil was baked in the oven for 10 min at ~300 °C. The dip−bake sequence was repeated eight times, after which the final coated foil was baked for 17 h at ~300 °C. The TiO_2 film thus built up on the Au surface had a thickness in the 0.5−1 μm range.

* To whom correspondence should be addressed. Telephone: 1-817-272-3810. Fax: 1-817-272-3808. E-mail: rajeshwar@uta.edu.

(1) Rajeshwar, K. *J. Appl. Electrochem.* **1995**, *25*, 1067.
(2) Rajeshwar, K.; Ibanez, J. *Environmental Electrochemistry*; Academic Press: San Diego, 1997.
(3) Blake, D. M. *Bibliography of Work on the Photocatalytic Removal of Hazardous Compounds from Water and Air*. NREL/TP-340-22197, National Renewable Energy Laboratory: Golden, CO, 1999. Update No. 4 to October 2001, NREL/TP-510-31319.
(4) Litter, M. I. *Appl. Catal. B. Environ.* **1999**, *23*, 89.
(5) Kraeutler, B.; Bard, A. J. *J. Am. Chem. Soc.* **1978**, *100*, 4317.
(6) Funt, B. L.; Tan, S.-R. *J. Polym. Sci.: Polym. Chem. Ed.* **1984**, *22*, 605.
(7) Okano, M.; Kikuchi, E.; Itoh, K.; Fujishima, A. *J. Electrochem. Soc.* **1988**, *135*, 1641.
(8) Yildiz, A.; Sobczynski, A.; Bard, A. J.; Campion, A.; Fox, M. A.; Mallouk, T. E.; Webber, S. E.; White, J. M. *Langmuir* **1989**, *5*, 148.
(9) Fox, M. A.; Worthen, K. L. *Chem. Mater.* **1991**, *3*, 253.
(10) Chenthamarakshan, C. R.; Ming, Y.; Rajeshwar, K. *Chem. Mater.* **2000**, *12*, 3538.
(11) Hodes, G.; Howell, I. D. J.; Peter, L. M. *J. Electrochem. Soc.* **1992**, *139*, 3136.

10.1021/cm049293b CCC: $27.50
Published on Web 08/31/2004

Instrumentation and Procedures. UV−visible spectra were recorded on a Hewlett-Packard model HP 8452-diode array spectrometer. Electron probe microanalysis (EPMA) was done on a JEOL JXA-8900R instrument with a beam voltage of 20 kV. X-ray photoelectron spectroscopy (XPS) used a Perkin-Elmer/Physical Electronics Model 5000C system. The photovoltammograms were acquired on a Model CV-27 BAS voltammograph instrument and recorded on a Soltec Model VP-6414S recorder. A 75 W xenon arc lamp (Oriel) served as the light source in these and in the chronopotentiometry (CP) experiments. For the linear sweep photovoltammetry experiments, chopped irradiation (chopping frequency = 0.2 Hz) from a 100 W tungsten−halogen lamp (Oriel) was used. In the chronopotentiometry and voltammetry experiments, the light source was 15 cm away from the TiO_2/Au working electrode surface, and the incident photon flux (as measured with an Oriel Model 70260 radiant power/energy meter) was in the range .95−2.2 mW/cm^2. For the CP experiments, the potential changes with the light on were monitored on a Soltec Model VP-6414S recorder. The time constant of this recorder was adequate for the slow, minute-scale temporal changes of interest here.

A 100 mL quartz beaker, TiO_2/Au working electrode, and a Ag|AgCl|satd KCl reference electrode inserted in the beaker served as the electrochemical cell for the CP experiments. A Pt spiral was additionally employed as the counter electrode for the photovoltammetry experiments. The supporting electrolytes in all the cases were prepurged with ultrapure N_2 prior to the experiments. A N_2 blanket was used during the two sets of experiments.

Photocatalytic deposition using TiO_2 powder dispersions used a medium-pressure (400 W) Hg lamp for photoexcitation and a quartz photoreactor as described elsewhere.[12,13] The Se^{IV} concentration in the aqueous dispersion was determined spectrophotometrically (analytical wavelength: 420 nm) using a derivatization method based on 3,3′-diaminobenzidine.[10,14] Procedures for removing solution aliquots for analyses from the photoreactor and for filtering out the TiO_2 particles have been described elsewhere.[15] Changes in the solution levels of both Cd^{II} and Pb^{II} were monitored spectrophotometrically at 494 and 520 nm, respectively, after derivatization with 4-(2-pyridylazo)resorcinol.[16]

The photocatalytic reduction of Cr^{VI} was done according to a procedure reported by us earlier.[17] In brief, the Cr^{VI}-loaded TiO_2 or CdSe−TiO_2 suspensions were equilibrated in the dark for 30 min. The difference between the initial concentration of Cr^{VI} (200 μM in the form of $Cr_2O_7^{2-}$) and the concentration at the end of the equilibration period (i.e., the initial concentration at zero time in Figure 10 below) was taken as the amount adsorbed on the TiO_2 particle surface in the dark. After this equilibration, the UV lamp was turned on, aliquots were syringed out periodically, and the solutions were analyzed for Cr^{VI} ions by measuring the absorbance at 352 nm on a UV−visible spectrophotometer after removing TiO_2 particles using PTFE syringe filters.

All the experiments described in this paper were performed on supporting electrolyte solutions or on aqueous dispersions of pH in the 6−7 range. The Se^{IV}-containing solutions were more acidic (pH ∼5); however, the pH changes after the photocatalysis experiments were negligible. Local pH changes were also negligible in the CP experiments. This trend is in contrast with the Cr^{VI} reduction case, where the pH changes can be appreciable, as elaborated elsewhere.[17] The use of buffers was intentionally avoided to preclude their interference with either the TiO_2 surface (e.g., phosphate species are notoriously interactive with the TiO_2 surface; for example, see refs 18−20) or the photochemistry/photoelectrochemistry extant in the aqueous media of interest. All the experiments here pertain to the ambient laboratory temperature (25 ± 3 °C).

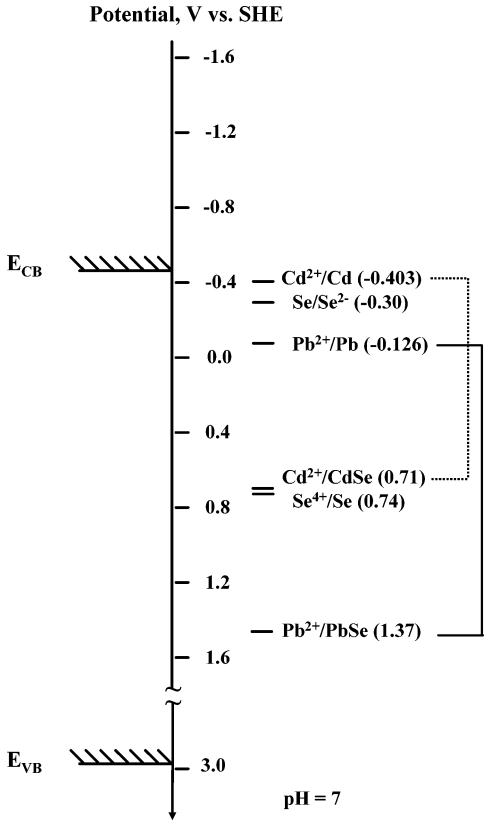

Figure 1. Relative disposition of the conduction and valence band-edges in TiO_2 and the redox energy levels for relevant species of interest to this study in an aqueous medium. Note the discontinuity in the potential scale at ∼1.6 V (vs SHE).

Results and Discussion

Photocatalytic Deposition of Se and MSe on the TiO_2 Surface. Figure 1 maps the relative disposition of the conduction and valence band edges in TiO_2 in an aqueous medium of pH ∼7. For comparison, the redox potentials of several species relevant to this study are also shown on the same diagram. The thermodynamic driving force for electron transfer from the oxide to an electron acceptor in solution (e.g., metal ions or Se^{IV} species) is given by the difference between the Fermi level of electrons in the oxide and the relevant redox potential in the contacting solution phase. On an irradiated oxide, the quasi-Fermi level of electrons moves in the negative direction to an ultimate location very close to the conduction band-edge of TiO_2. We assume here that "hot" carrier effects can be neglected. Thus, there is no thermodynamic driving force for the direct reduction of Cd^{2+} ions by the photogenerated electrons in TiO_2, while that for the photocatalytic reduction of Pb^{2+} species is modest.[10] On the other hand,

(12) Lin, W.-Y.; Wei, C.; Rajeshwar, K. *J. Electrochem. Soc.* **1993**, *140*, 2477.
(13) Lin, W.-Y.; Rajeshwar, K. *J. Electrochem. Soc.* **1997**, *144*, 2751.
(14) Chenthamarakshan, C. R.; Yang, H.; Savage, C. R.; Rajeshwar, K. *Res. Chem. Intermed.* **1999**, *25*, 861.
(15) Chenthamarakshan, C. R.; Rajeshwar, K. *Electrochem. Commun.* **2000**, *2*, 527.
(16) Chenthamarakshan, C. R.; Yang, H.; Ming, Y.; Rajeshwar, K. *J. Electroanal. Chem.* **2000**, *494*, 79.
(17) Chenthamarakshan, C. R.; Rajeshwar, K.; Wolfrum, E. J. *Langmuir* **2000**, *16*, 2715. See references therein.
(18) Abdullah, M.; Low, G. K.-C.; Mathews, R. W. *J. Phys. Chem.* **1990**, *94*, 6820.
(19) Connor, P. A.; McQuillan, A. J. *Langmuir* **1999**, *15*, 2402.
(20) Kajitvichyanukul, P.; Chenthamarakshan, C. R.; Rajeshwar, K.; Qasim, S. R. *Adsorp. Sci. Technol.* **2003**, *21*, 217. See also references therein.

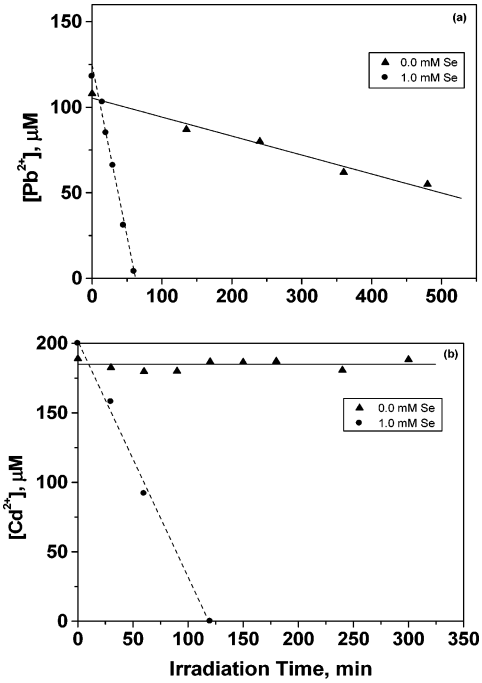

Figure 2. (a) Photocatalytic reduction of 200 μM Pb^{II} in N_2-purged TiO_2 suspensions (2 g/L TiO_2 dose) under UV irradiation. In the 1.0 mM Se case, the TiO_2 suspension containing 1.0 mM Se^{IV} species was preirradiated for 30 min before it was dosed with 200 μM Pb^{II} species. (b) As in panel a but for the photocatalytic reduction of 200 μM Cd^{II} species. See Experimental Section for details. The lines are least-squares fits of the data points.

there is appreciable driving force for the photoreduction of Se^{IV} species (Figure 1). As Figure 2 and the data presented earlier on Se^{IV} reduction in ref 10 illustrate, these predictions are very well borne out by experiment. Thus, no reduction of Cd^{2+} is observed in a UV-irradiated TiO_2 aqueous dispersion over a ~6 h period (Figure 2b). Lead(II) species are photoreduced very slowly over a 10 h timespan via a zero-order kinetics reaction (Figure 2a). On the other hand, Se^{IV} species have a strong adsorptive affinity for the TiO_2 surface and are photoreduced in a facile manner.[10]

The crucial aspect with the photoassisted deposition of MSe on the TiO_2 surface is that the free energy of compound formation (ΔG_{MSe}) effectively shifts the redox potentials in the $Cd^{2+/0}$ and $Pb^{2+/0}$ cases in the positive direction (Figure 1). This shift is somewhat larger in the PbSe case relative to CdSe because of the more favorable ΔG_{MSe} value, −264.5 kJ/mol for PbSe vs −136.4 kJ/mol for CdSe (refs 21, 22). Thus on a Se-modified TiO_2 surface, the reduction of Cd^{2+} and Pb^{2+} species is driven by compound formation in much the same manner that metal alloys are deposited. Once again, experimental data (Figure 1) are in accord with these expectations. The solutions are depleted of Cd^{2+} (Figure 2b) and Pb^{2+} (Figure 2a) ions within ~120 and ~60 min, respectively, when the TiO_2 particle surfaces are modified with selenium.

The above two examples comprising of the Cd−Se and Pb−Se systems (and elaborated further by eqs 1 and 2)

$$Se + M^{2+} + 2e^- \xrightarrow[h\nu]{TiO_2} MSe_{(TiO_2)}\ (M = Cd, Pb) \quad (1)$$

$$M^{2+} + 2e^- \xrightarrow[h\nu]{TiO_2} M_{(TiO_2)}\ (\text{unfavorable}) \quad (2)$$

represent good test cases of situations where the *thermodynamic* predictions and the observed *kinetics* trends are entirely in accord with one another. Note that the faster photoreduction in the Pb−Se case (Figure 2a) is consistent with the larger driving force for the Pb^{2+}/PbSe redox case relative to the Cd^{2+}/CdSe (Figure 2b) counterpart.

The "TiO_2" (or "Se") subscripts within parentheses in eqs 1 and 2 (and in the other equations below) denote the parent phase where the participating species are located. What about the mechanism of MSe formation on the TiO_2 surface? Either an "ionic" (eqs 3, 4, and 7) or "atomic" (eqs 5−7) pathway can be envisioned.

Ionic:

$$Se_{(TiO_2)} + 2e^-_{(TiO_2\ or\ Se)} \rightarrow Se^{2-}_{(TiO_2)} \quad (3)$$

$$M^{2+}_{(aq)} + Se^{2-}_{(TiO_2)} \rightarrow MSe_{(TiO_2)} \quad (4)$$

Atomic:

$$M^{2+}_{(aq)} + 2e^-_{(TiO_2)} \rightarrow M_{(TiO_2)} \quad (5)$$

$$M_{(TiO_2)} + Se_{(TiO_2)} \rightarrow MSe_{(TiO_2)} \quad (6)$$

Overall

$$M^{2+}_{(aq)} + Se_{(TiO_2)} + 2e^- \rightarrow MSe_{(TiO_2)} \quad (7)$$

Chronopotentiometry (CP) experiments[23] were designed to address this aspect and are presented next.

Chronopotentiometry Probes of Se Deposition and MSe Formation on the TiO_2 Surface. In these experiments, the potential of the TiO_2 film substrate (versus a suitable reference electrode) is monitored in the dark and when the excitation light is turned on. Charge accumulation and transfer processes at the TiO_2 film/solution interface subsequently influence the temporal evolution of the TiO_2 film potential, as elaborated elsewhere.[23] Figure 3 contains representative data; CP profiles during Se^{IV} photoreduction and in a control run where the Se^{IV} species were omitted from the supporting electrolyte (0.05 M Na_2SO_4) are compared and contrasted. In the control run, the potential moves in the negative direction when light is turned on. This is consistent with the accumulation of photogenerated electrons on the TiO_2 surface, i.e., the interface undergoes charging much like in a capacitor.[23] Subsequently, these electrons are trapped in surface sites and the potential relaxes back to a stable plateau around −0.1 V. Note that there are no intentionally added redox species in the electrolyte to scavenge the photogenerated electrons in this case. Protons are present in the electrolyte, albeit at very low concentrations; however,

(21) Mishra, K. K.; Rajeshwar, K. *J. Electroanal. Chem.* **1989**, *273*, 169.

(22) For data for the calculation of ΔG_f^0 for PbSe, see: *CRC Handbook of Chemistry and Physics*, 1st student ed.; CRC Press: Boca Raton, FL, 1988; pp D35-D77.

(23) Sun, W.; Chenthamarakshan, C. R.; Rajeshwar, K. *J. Phys. Chem. B* **2002**, *106*, 11531.

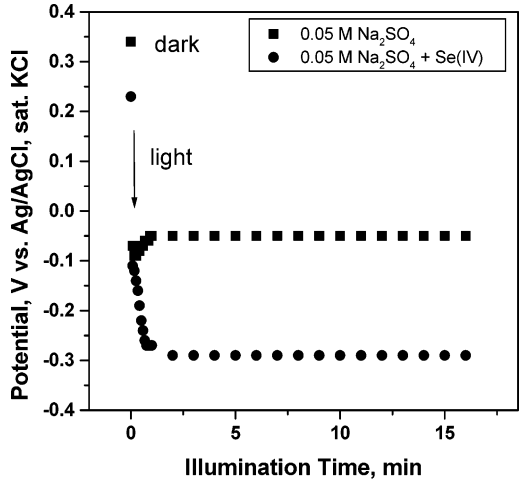

Figure 3. Chronopotentiometric (CP) profiles for a UV-irradiated TiO_2 film electrode in contact with 0.05 M Na_2SO_4 supporting electrolyte with and without added Se^{IV} (at 200 μM level) species.

the TiO_2 surface is not intrinsically catalytic toward proton reduction.[1,2]

When Se^{IV} species are present in the electrolyte, the TiO_2 film potential is pinned at ca. −0.30 V (Figure 3). Interestingly, this potential is located in the range of the $Se^{0/2-}$ redox potential (Figure 1). This is strong support for the ionic mechanism (see eq 3 above). Further support is furnished by the linear sweep photovoltammetry data to be presented below. That Se^{IV} reduction proceeds beyond the initial $4e^-$ step (leading to elemental Se) is also suggested by the work of another group.[24] These authors have invoked a p−n junction model for the TiO_2/Se interface that explicitly considers the p-type semiconductor nature of Se and the consequent ease of its further photoreduction (to Se^{2-}).[24]

Figure 4 contains further CP data on the Cd−Se system. Two of the CP profiles are reproduced here from Figure 3 for direct comparison. Also shown are two control runs where the 0.05 M Na_2SO_4 supporting electrolyte was dosed with Cd^{II} species. These data are virtually superimposable on the blank run, reaffirming the lack of redox activity of Cd^{II} species with the UV-irradiated TiO_2 surface (cf., Figure 2b). On the other hand, when the Cd^{II} species are dosed into the electrolyte in contact with a Se-modified TiO_2 surface, the CP profile is markedly different (inverted triangles, Figure 4). The potential is still pinned in the negative regime, but there is a *small, but reproducible* positive shift of the plateau potential relative to the Se^{IV} case (cf., the two sets of data marked by normal and inverted triangles in Figure 4). This positive shift is a direct, experimental manifestation of the "alloy" effect discussed earlier related to the ability of Cd^{II} species to exchange charge with the Se-modified TiO_2 surface.

Figure 5 contains CP profiles for the Pb−Se system. The supporting electrolyte was switched from Na_2SO_4 to NaCl because of the limited solubility of Pb^{2+} ions in the former case. The data represented by open circles and closed squares up to 30 min are for the control cases, where the photogenerated electrons in TiO_2 are simply trapped by the surface sites (see above). Consider

(24) Tan, T. T. Y.; Zaw, M.; Beydoun, D.; Amal, R. *J. Nanoparticle Res.* **2002**, *4*, 541.

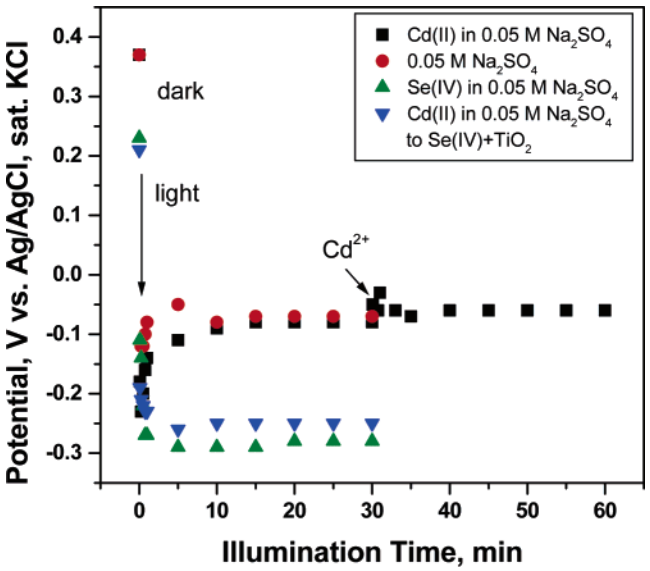

Figure 4. CP profiles for experiments involving Cd^{II} species. The two sets of data from Figure 3 (triangles and circles) are reproduced here for direct comparison. Additionally, a control run or Cd^{II} species in 0.05 M Na_2SO_4 is shown (squares). In another control run, Cd^{II} species were dosed (at 200 μM level) into the 0.05 M Na_2SO_4 electrolyte after 30 min of irradiation (indicated by the arrow in Figure 4). In the fifth experiment, Cd^{II} species were added (at 200 μM level) at the inception of the run and the TiO_2 film was pre-modified with Se (see text).

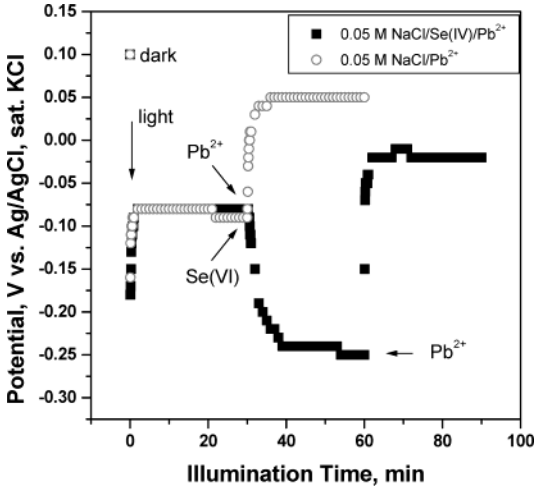

Figure 5. As in Figure 4 but for Pb^{II} species. The supporting electrolyte was 0.05 M NaCl instead of 0.05 M Na_2SO_4. The data up to 30 min are from two identical runs and illustrate the degree of reproducibility in the CP profiles. At 30 min (open circles), Pb^{II} species were dosed in (at 200 μM level). Similarly, in the other experiment (data denoted by closed squares), Se^{IV} species were dosed in at 30 min (at 200 μM level) and Pb^{2+} species at 60 min (at 200 μM level).

the CP profile represented by the open circles first. When Pb^{II} species are dosed in, the potential immediately shifts in the positive direction and attains a new plateau around ~0.05 V. Recall that Pb^{2+} ions are capable of exchanging charge (i.e., being photoreduced) by UV-irradiated TiO_2 (cf., Figure 2a).

On the other hand, when Se^{IV} species are dosed in at 30 min (filled squares, Figure 5), the potential shifts in the negative direction as before (cf., Figures 3 and 4). Now when Pb^{2+} ions are *also* additionally dosed in after 60 min, the TiO_2 film potential undergoes a marked

positive shift, signaling Pb^{2+} reduction *and* Pb−Se compound formation. Note that the extent of this shift far exceeds the case where Se species are absent at the TiO_2/electrolyte interface. The shift is also much more pronounced relative to the Cd−Se system (cf., Figures 4 and 5). All these trends are consistent with the relative thermodynamic driving forces (Figure 1) and the faster kinetics in the Pb−Se system relative to the Cd−Se counterpart (cf., bottom sets of data in Figure 2a,b). Many of the trends seen in the CP profiles above can also be rationalized on the basis of the "mixed potential" concept borrowed from the corrosion field. Namely, a photocatalytic system at open-circuit adopts a "null" potential such that the anodic and cathodic current branches balance one another.[25] In the absence of a depolarizer in the solution, on the other hand, the photogenerated electrons simply accumulate within the TiO_2 surface, charging it up.

Linear Sweep Photovoltammetry Using Visible Light Excitation of Se- and CdSe-Modified TiO_2 Electrodes. In linear sweep photovoltammetry, interrupted photoexcitation of a (semiconductor) electrode is employed during a slow (e.g., 2 mV/s) potential sweep.[21,26,27] Thus the current−potential profile can be mapped in the same experiment for a given electrode material both in the dark and under electrode illumination. n-Type semiconductors exhibit photoenhancement of current in the anodic direction, while the opposite trend (photocathodic current flow) holds for p-type semiconductors. Figure 6 contains linear sweep photovoltammogram (LPV) traces for a Se-modified TiO_2 film (Figure 6a) and a CdSe/TiO_2 film counterpart (Figure 6b). Cartoons of the electrode morphologies in the two cases are also depicted in these figures. Visible light photoexcitation was employed so that the contribution from the underlying TiO_2 substrate could be minimized. (Recall that the optical band gap of Se and CdSe are much smaller than that of TiO_2).[26]

When the potential is swept in the positive direction from a negative value (ca. −0.40 V) (see Figure 6a), the p-type Se sites on the TiO_2 surface (separate microscopy data reveal that the Se phase does not form a *continuous* layer on the TiO_2 surface) are under reverse bias. Thus, after photoexcitation of electron−hole pairs in Se, the electrons are driven by the electric field to the solution interface. There these carriers can participate in photocathodic processes, namely, the reduction of Se itself (cf., Figure 3), protons, or even adventitious dissolved O_2 in the contacting electrolyte. The spikes seen especially in Figure 6a are diagnostic of facile carrier recombination. That the Se layer formed from the reduction of Se^{IV} species acts as a p-type semiconductor is demonstrated by the LPV data in Figure 7. The photocathodic enhancement of current flow as the potential is swept negative past the flatband potential at ∼0.2 V (reverse bias regime for a p-type semiconductor) (Figure 7) is diagnostic of p-type semiconductor behavior.[21] Past a potential of ca. −0.10 V in the *other direction* (see Figure 6a), the imposed potential manifests as a reverse bias across the (underlying) TiO_2 regions. This results in *photoanodic* current flow resulting from the movement of photogenerated holes in TiO_2 across the interface and their participation in either the oxidation of hydroxyl groups on the oxide surface or of bulk water molecules.

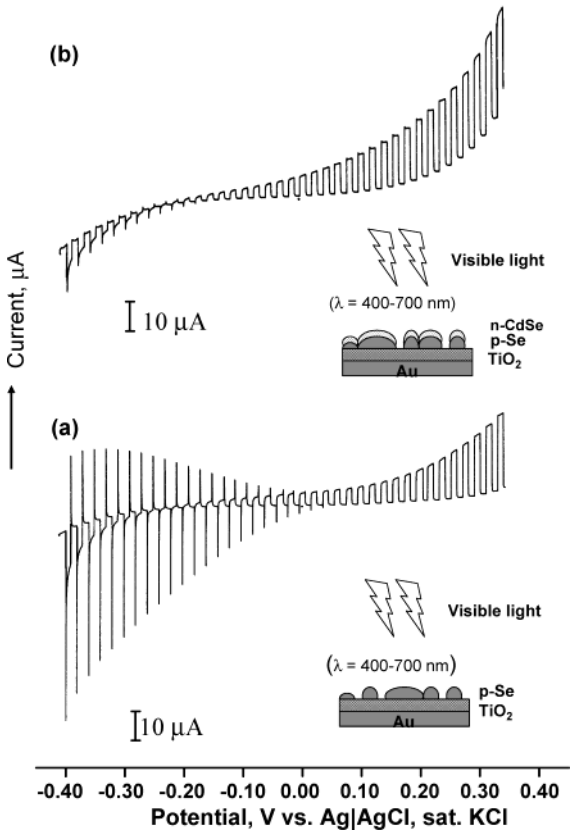

Figure 6. Linear sweep photovoltammograms in 0.5 M Na_2SO_4 for (a) Se-modified TiO_2 film and (b) CdSe- and Se-modified TiO_2 film (see the text). The potential scan rate was 2 mV/s and the geometric area of the film was 0.8 cm^2. Visible light irradiation was employed, unlike in the experiments in Figures 2−5 above.

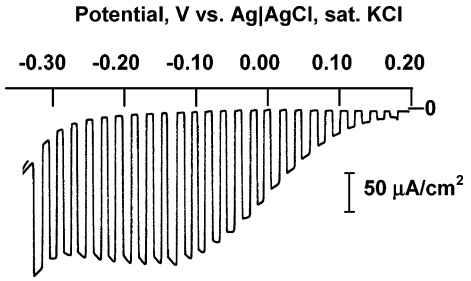

Figure 7. Photovoltammogram for an electrodeposited Se^0 film in 0.5 M H_2SO_4. The Se film was grown on a gold surface by polarizing for 15 min at −0.7 V (vs Ag|AgCl) in a solution containing 10 mM SeO_2 in 0.1 M Na_2SO_4. Other conditions are as in Figure 6.

Most significantly, on a p-Se film on *gold* substrates (Figure 7), the photopotential attained is not negative enough to drive the $Se^0 \rightarrow Se^{2-}$ cathodic process, and thus MSe formation is precluded on an irradiated p-Se/Au electrode *at open circuit*.[28] These findings furnish additional evidence in support of the ionic mechanism for MSe compound formation on the irradiated TiO_2 surface (see above).

(25) Rajeshwar, K.; Ibanez, J. G. *J. Chem. Educ.* **1995**, *72*, 1044.
(26) Frese, K. W., Jr. *J. Appl. Phys.* **1982**, *53*, 1571.
(27) Da Silva Pereira, M. I.; Peter, L. M. *J. Electroanal. Chem.* **1982**, *131*, 167.
(28) de Tacconi, N. R.; Rajeshwar, K. To be published.

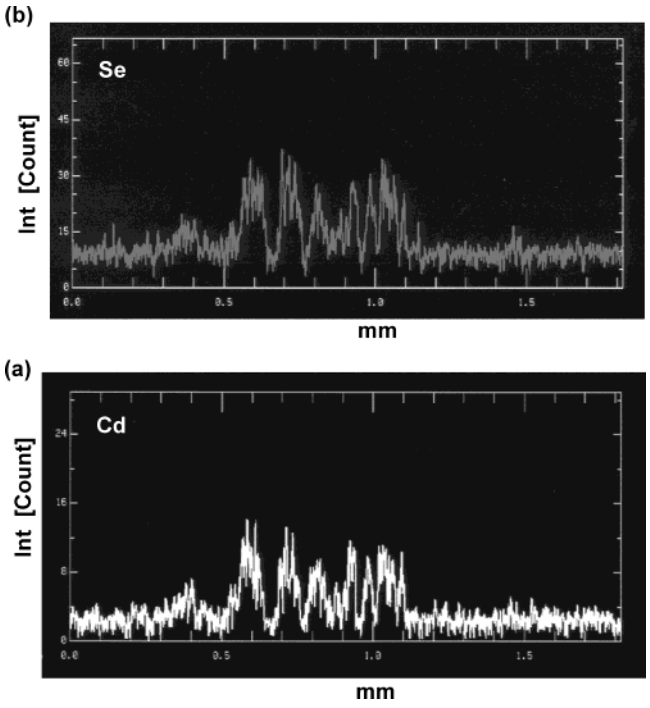

Figure 8. Representative EPMA elemental map for a sample as in Figure 6b. A mask was used to delineate the areas on the TiO_2 surface for Se and CdSe deposition (see the text). The analytical electron beam was then rastered across these selected spots, one example of each being shown in the profiles in Figure 8.

When the Se sites are partially converted to CdSe, two trends in the LPV profiles are striking (Figure 6b). First, the photocathodic envelope is much diminished in amplitude (relative to that in Figure 6a) because of the conversion of many of the surface p-type Se sites to n-CdSe. Second, the *photoanodic* portion is somewhat amplified, because now *both* n-CdSe and n-TiO_2 respond to the visible photoexcitation, unlike the case in Figure 6a, where only n-TiO_2 is present.

Bipolar LPV profiles (i.e., photovoltammograms exhibiting photocathodic and photoanodic behavior in the same trace) such as those in Figure 6 are not commonplace in the semiconductor electrochemistry literature.[11,29] This interesting behavior is possible in the composite semiconductor structures such as those considered in Figure 6 because the n-type and p-type semiconductor regions can be separately accessed by the electrolyte. In fact, in the structure in Figure 6b, one p-type semiconductor (Se) is in electronic contact with two n-type semiconductor (TiO_2 and CdSe) components, reminiscent of a n−p−n (transistor-like) configuration. We have recently developed similar electrode structures wherein n- or p-type behavior can be instigated by switching from UV−to visible-light photoexcitation.[30]

Ex Situ Characterization of Se- and CdSe-Modified TiO_2 Surfaces. Figure 8 contains representative electron probe microanalysis (EPMA) elemental maps for Cd (Figure 8a) and Se (Figure 8b) for a CdSe/TiO_2 film with the morphology schematized as an insert in Figure 6b; i.e., the film has a CdSe/Se/TiO_2 configuration. A custom-made mask containing 0.7 mm diameter holes was used on top of the TiO_2 surface to delineate the regions for Se and CdSe deposition. Specifically, the mask was used to selectively deposit individual "spots" on the TiO_2 surface that could then be converted to the metal selenide. The EPMA probe was rastered across these spots for elemental analyses. Figure 8 shows the results for the CdSe/TiO_2 case. Significantly, the spatial distribution of the two elements on the parent TiO_2 is highly correlated, the Cd signals mimicking their Se counterparts in Figure 8. This is yet another strong piece of evidence for the deposition model considered earlier; namely, that Cd deposition is induced by the Se on the TiO_2 surface.

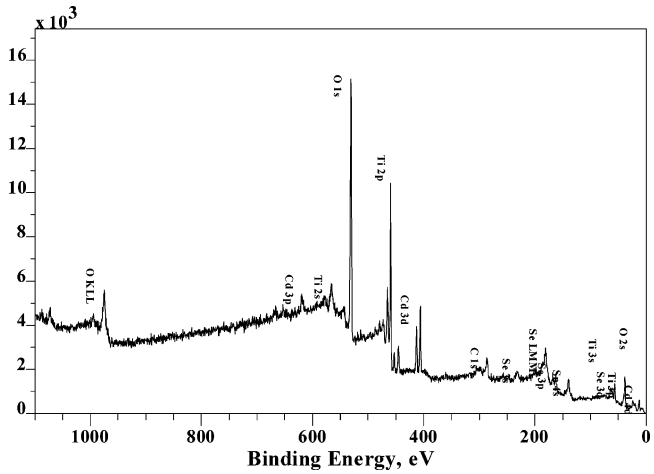

Figure 9. Survey XPS scan for a sample as in Figure 6b.

Figure 9 contains a survey XPS spectrum of a sample very similar to that considered above in Figures 6b and 8. Aside from the (expected) TiO_2 signals, peaks assignable to both Cd and Se are clearly seen. High-resolution XPS data provide further support for the chemical composition of both the MSe/TiO_2 composites. The PbSe/TiO_2 sample gave a Pb $4f_{7/2}$ binding energy value of 138.2 eV compared with 138.3 eV for an authentic sample of PbSe.[31] The Se 3d binding energy value in PbSe/TiO_2 was 54.3 eV versus 53.9 eV for the authentic sample of PbSe. Values of 405.3 eV for Cd $3d_{5/2}$ and 55.2 eV for Se 3d were obtained for CdSe/TiO_2 compared to 405.7 and 54.9 eV, respectively, for an authentic sample of CdSe.[31] For comparison, the 3d binding energy in elemental Se is 55.5 eV for an authentic sample of Se.[31]

Application of CdSe/TiO_2 in Cr^{VI} Remediation. A key step in the environmental remediation of carcinogenic Cr^{VI} is its reduction to the much less mobile Cr^{III} state.[17] We[17] and others[32] have deployed TiO_2 for the photocatalytic remediation of Cr^{VI} in aqueous streams. Figure 10 compares the Cr^{VI} conversion profiles for TiO_2 and CdSe-modified TiO_2 powders in N_2-purged and UV-irradiated aqueous dispersions. Contrasting with the behavior of the parent TiO_2, all of the Cr^{VI} initially present is photoreduced within ~5 min on the CdSe/TiO_2 surface. We attribute this greatly ac-

(29) de Tacconi, N. R.; Carmona, J.; Rajeshwar, K. *J. Phys. Chem. B* **1997**, *101*, 10151.
(30) de Tacconi, N. R.; Chenthamarakshan C. R.; Rajeshwar, K. **2004**, to be published.
(31) Wagner C. D.; Riggs, W. M.; Davis, L. E.; Mulder, J. F.; Mattenberg, G. E. *Handbook of X-ray Photoelectron Spectroscopy*, Perkin-Elmer Corp. (Physical Electronics Division): Eden Prairie, MN, 1979. The authentic samples were PbSe (Aldrich, 99.999%), CdSe (Aldrich, 99.99%), and Se (Alfa Aesar, 99.999%), respectively.
(32) Prairie, M. R.; Evans, L. R.; Stange, B. M.; Martinez, S. L. *Environ. Sci. Technol.* **1993**, *27*, 1776. See references therein.

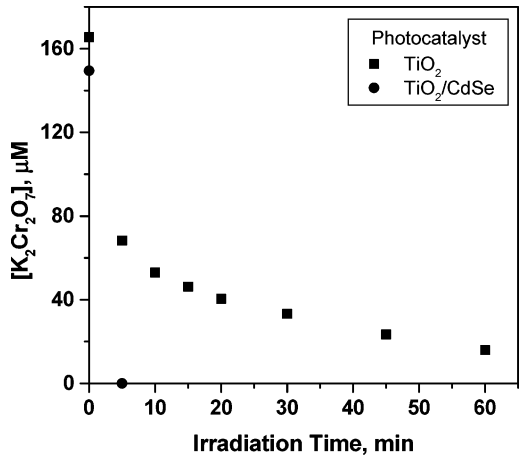

Figure 10. Photocatalytic reduction of 200 μM $K_2Cr_2O_7$ in N_2-purged TiO_2 and TiO_2/CdSe suspensions. See Experimental Section for details.

celerated photocatalytic activity to vectorial electron transfer and minimized carrier recombination in CdSe/TiO_2 relative to TiO_2. The CdSe/TiO_2 samples presumably also have an enhanced absorption cross section of the UV lamp output (relative to TiO_2) because of the additional absorption by the CdSe counterpart (cf., Figure 6b). This must be carefully quantified in separate experiments. Further, we have not yet studied: (a) the local pH changes in the two instances in Figure 10, (b) the fate of the photogenerated holes, and (c) the long-term stability of the CdSe/TiO_2 particles under UV or visible irradiation. Previous studies[33] on composite CdSe/TiO_2 samples prepared by other methods suggest that the photogenerated holes and electrons are localized in the TiO_2 and CdSe phases respectively, but this needs to be verified. We also have intervening (unconverted) Se regions in our composite particles (see above) that surely play a role in mediating charge transfer or storage. However, these issues fall beyond the scope of the present study.

(33) Liu, D.; Kamat, P. V. *J. Phys. Chem.* **1993**, *97*, 10769.

Concluding Remarks

We have built on an earlier proof-of-concept study[10] that demonstrated the feasibility of preparing Se- or MSe-modified TiO_2 surfaces using heterogeneous photocatalysis. Indeed, this is a general preparative strategy that should be applicable to other semiconductors besides TiO_2. One important requirement is that the "host" semiconductor is photoelectrochemically stable in aqueous media. The photogenerated electrons must also have sufficient energy and good kinetics for electrochemically reducing the second semiconductor component (such as Se) onto its surface. The composite synthesis can be completed by choosing an (electropositive) element capable of alloying with the deposited element on the host semiconductor surface. Two such species (Pb^{II} and Cd^{II}) were considered in this study, but other candidates are worth exploring in the future.

Acknowledgment. This study was supported in part by a grant from the U. S. Department of Energy, Office of Basic Energy Sciences. We thank Prof. R. Shiratsuchi (Kyushu Institute of Technology, Japan) for the EPMA data, and the three (anonymous) reviewers for constructive criticisms of an earlier version of the manuscript.

CM049293B